MATHEMATICAL HUMAN BODY MODELS REPRESENTING A MID SIZE MALE AND A SMALL FEMALE FOR FRONTAL, LATERAL AND REARWARD IMPACT LOADING

R. Happee[1,3], S. Ridella[2], A. Nayef[2], P. Morsink[1], R. de Lange[1], R. Bours[1,3], J. van Hoof[1]

[1] TNO Automotive, The Netherlands; [2] TRW Vehicle Safety Systems, Michigan, US;
[3] Eindhoven University of Technology, The Netherlands

ABSTRACT

A human body model representing a mid size male has been presented at the 1998 STAPP conference. A combination of modelling techniques was applied using rigid bodies for most segments, but describing the thorax as a deformable structure. In the current paper this modelling strategy was employed to also develop a model representing a small female. The validation database was extended and now also includes lateral validation. The anthropometry of both models has been derived from the RAMSIS anthropometry database. Joint properties for the mid size male were derived from literature, and established scaling techniques were employed to derive joint properties for the small female model.

The mid size male model was validated using: frontal volunteer sled tests, frontal and lateral post mortem human subject (PMHS) impactor tests in various body regions, lateral PMHS sled tests, and rearward volunteer and PMHS tests. The small female model was validated using scaled biofidelity requirements from the literature and biomechanic data of the applicable body size including side airbag loading. The models were found to satisfy the available biofidelity requirements in terms of kinematics, chest deflections, and accelerations.

Keywords: Biomechanics, Multi Body, Human Models, Cadavers, Volunteers, Validation

THE CURRENT CRASH-SAFETY DESIGN AND RESEARCH is largely based on mechanical human body models (crash dummies). In addition to mechanical testing, mathematical modelling is widely used. However, most occupant models used in crash simulations are based on dummies and thereby inherit apparent differences between dummies and the real human body. Mathematical modelling of the real human body potentially offers improved biofidelity and allows the study of aspects like body size, posture, muscular activity and post fracture response. Detailed human body modelling potentially allows analysis of injury mechanisms on a material level.

A large number of models describing specific parts of the human body have been published but only a few of these models describe the response of the entire human body in impact conditions. Models simulating the response of car occupants have been published for lateral loading (Huang et al., 1994a, 1994b; Irwin, 1994), frontal loading (Ma et al., 1995), and rearward loading (Jakobsson et al., 1994, Kroonenberg et al., 1997). Lizee et al. (1998) validated an occupant model for frontal and lateral loading. A model for vertical loading has been published by Prasad and King (1974) and pedestrian models have been published by Ishikawa et al. (1993) and Yang et al. (1997).

The application and validation of the above-mentioned human models is limited to specific loading directions. A human body model representing a mid size male for multi-directional impact loading has been presented in a previous paper (Happee et al., 1998). A combination of modelling techniques was applied using rigid bodies for most segments, but describing the thorax as a deformable structure. In the current paper this modelling strategy was employed to also develop a model representing a small female and both models were extended and validated for lateral loading. This validation includes a range of impactor tests, sled tests on the mid size male and a side airbag test on the small female.

MODEL SETUP

The model has been developed aiming at omni-directional biofidelity where the highest priority was given to the torso and the head-neck system. The model has to provide a biofidelic interaction with the seat back, which requires a realistic surface description for pelvis, spine, thorax, neck and head. The whole spine has to be biofidelic in forward/rearward as well as lateral bending, but also in compression/elongation and the surface description of the model has to be coupled realistically to the spinal model. For all loading directions an accurate prediction of head kinematics and neck loads is needed. For frontal impact the model has to provide a biofidelic interaction with belts and airbags which requires an accurate surface description for the frontal area of upper and lower torso. Especially for the sternal area a realistic prediction of the chest deflection is needed. To provide realistic interactions with car interiors and airbags during lateral impact the model has to predict biofidelic lateral kinematics on the level of shoulder, thorax, abdomen and pelvis.

The model was set up for optimal efficiency and robustness. This has been achieved using multi body techniques available in MADYMO version 5.4. Most skeletal structures have been modelled as rigid bodies connected by joints. Deformation of the rib cage has been accomplished using flexible bodies (Koppens et al., 1993) and the outer skin has been implemented as an "arbitrary surface". The lumped joint resistance resulting from ligamentous and muscular tissues has been implemented using non-linear stiffness functions and energy dissipation was implemented using hysteresis or damping.

ANTHROPOMETRY

In the area of vehicle crash-safety design, limited attention is being paid to variations of body size. For adults, current regulations prescribe testing with dummies representing a "50th percentile male" only. For frontal impact two other dummy sizes are available representing a small female (5th percentile) and a large male (95th percentile) (Mertz et al., 1989). A small female dummy for side impact has been introduced as well (Daniel et al., 1995). Due to the time and cost involved in design and production of new physical dummies, the number of available dummy sizes will remain limited. Where the current dummy sizes do represent variations in length and the associated body mass they do not cover variations in body proportions. Published anthropometric human body models do describe such variations in body proportions. As motivated in Happee et al. (1998) the RAMSIS model has been selected as main anthropometry source. RAMSIS has primarily been developed for ergonomic analyses and allows the generation of models with a wide range of anthropometry parameters. The RAMSIS model describes the human body as a set of rigid bodies connected by kinematic joints and the skin is described as a triangulated surface. RAMSIS provides a detailed geometric description of the body segments based on extensive anthropometric measurements on various civilian populations including automotive seated postures. A translator has been developed to convert RAMSIS models in any body size into MADYMO models.

In addition to the mid size male model described by Happee et al. (1998), now a small female model was developed. Comparable to the Hybrid III and the SID2s 5th percentile female dummies, this small female human model was defined small with respect to both length and weight (see Appendix A). The RAMSIS human models were converted to MADYMO which provided: joint locations, joint ranges of motion, segment masses and centres of gravity, and a triangulated skin connected to various body segments. This model was extended as follows. Rotational inertia was derived by integration over segment volume where for each segment a homogeneous density was assumed. Joint resistance models were added and the vertebrae were modelled as rigid bodies connected by joints allowing rotations as well as translations. The required additional parameters for the male model were based on biomechanic data from the literature (see further Happee et al., 1998). These parameters were verified by validation of the complete male model. Then these parameters were scaled for application in the small female model. Scaling procedures have been used widely in the field of crash safety. The design of the Hybrid III small female and large male dummies is partly based on scaling (Mertz et al., 1989) and biofidelity requirements for adults have been used to estimate requirements for children (van Ratingen, 1997; Irwin and Mertz, 1997).

Based on the known anthropometry parameters, scaling supplied joint characteristics (stiffness, friction, damping and hysteresis), contact characteristics and all other force models. Established scaling rules have been applied where for the current adult models it has been assumed that material properties are invariant with subject size.

THORAX

In impact the human thorax deforms in a complex 3D manner due to contacts, but also due to spinal deformations. Deforming thorax models have been developed using finite elements but the resulting calculation times are a major drawback for common applications. Therefore MADYMO flexible bodies have been applied (Koppens, 1993). These flexible bodies (or super elements) describe 3D deformations with only a few degrees of freedom and are therefore extremely efficient.

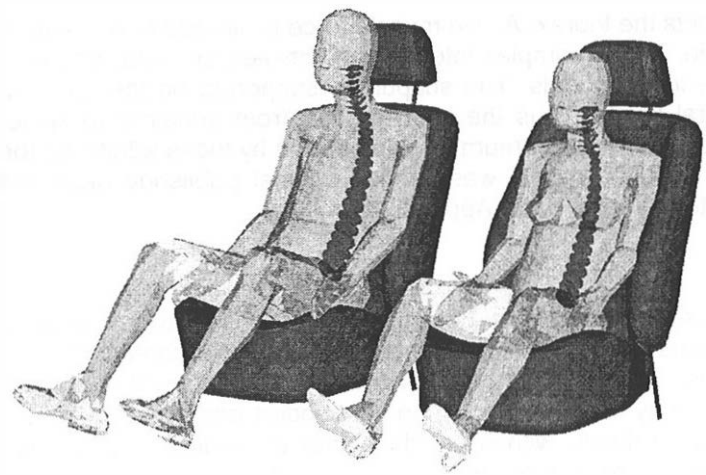

Fig. 1: Human models representing a mid size male (left) and a small female (right).

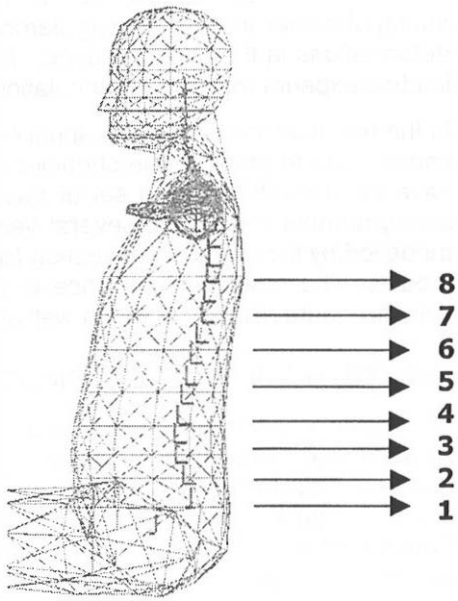

Fig. 2: Flexible body positions in the thorax and abdomen region.

The geometry of the flexible bodies is described by a number of nodes to which point masses are assigned. These nodes also support the arbitrary surface skin. The human torso skin is divided in 8 parts supported on 8 flexible bodies shown in Fig. 2. The flexible bodies are supported at the spine at the closest vertebral body. For each flexible body, the degrees of freedom are predefined to represent 3D deformation patterns (or modes). In the current model, each flexible body contains one frontal mode and two identical lateral modes. The actual deformations are linear superpositions of the defined modes. Fig. 3 shows resulting deformation patterns of an isolated deformable torso segment for frontal and lateral loading. The flexible bodies describe global deformations while the contact algorithm describes local deformation. The resulting capability to model torso deformation was found sufficient to match the available validation data.

Spring damper models (point restraints) are attached between the flexible bodies and the spine and in between the flexible bodies. These provide frontal and lateral non-linear stiffness and damping to match impactor biofidelity requirements (see validation in Appendix B) in a comparable way as the Lobdell model (Lobdell, 1973). Furthermore they provide coupling and load sharing between the flexible bodies. The two lowest flexible bodies contain the iliac wings. Since no biomechanic data was available the resistance for frontal loading of these two lowest deformable sections is based on a model of the Hybrid III 50th percentile dummy.

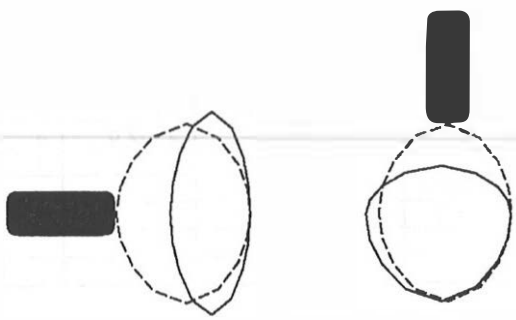

Fig. 3: Deformation patterns of an isolated torso flexible body in frontal compression (left) and lateral compression (right), the undeformed state is also plotted in both figures.

SHOULDERS

The shoulder mechanism forms a moving base for the upper extremity. It contains a number of joints connecting the humerus, the scapula, the clavicle and the sternum. Furthermore, the scapula contacts the back of the thorax; it can glide over the so-called scapulothoracic gliding plane. This connection makes the shoulder a closed chain mechanism. In the model the clavicle, scapula and humerus are represented as rigid bodies which are connected by spherical joints. The rotational joint characteristics are based on biomechanic data by Engin (1980). The clavicles the sternum and the rib cage deform during shoulder loading. Spring-damper models between the clavicle and sternum bodies incorporate deformations in the shoulder girdle. The deformation characteristics are based on PMHS axial clavicle loading experiments and FE simulations of clavicle and rib cage.

In the real human body, the scapula contacts the thorax. Active muscle force is needed to maintain this contact and to stabilise the shoulder girdle. These complex interactions between shoulder and thorax have been modelled as a set of passive force models. The scapula is supported on the spine with spring-damper models at several vertebral levels. Thus the load transfer from shoulder to spine is modelled by the skeletal connection (scapula-clavicle-sternum-ribs-spine) and by these additional force models. The resulting resistance of the shoulder model was verified against published quasi-static volunteer data (Engin, 1980) as well as lateral impact data (Appendix B).

ARBITRARY SURFACE DESCRIPTION

Traditional contact algorithms used in crash simulations describe interactions between analytical surfaces like ellipsoids, planes and cylinders, and also finite elements. Recently a contact algorithm has been developed for " arbitrary surfaces" (MADYMO, 1999). Arbitrary surfaces consist of triangular or quadrangular facets, which are supported by nodes (vertices) on rigid bodies and/or flexible bodies. Contact can be specified with other arbitrary surfaces, with ellipsoids, planes and cylinders or with finite elements. In these contacts the compliance of the materials is taken into account by allowing penetrations in the contacting surfaces. For each node of the facet surface the local contact stress is calculated applying a user-defined function of the penetration. The contact force on each node is obtained by multiplying the calculated contact stress by the area around the node. This contact force is transferred from the surface model to the applicable rigid body or flexible body.

The outer surface of our human model (skin) is described as an arbitrary surface consisting of around 2000 triangular facets connecting around 1000 vertices (nodes). This surface is largely supported by rigid bodies. However, in the thorax area the skin is supported by flexible bodies. This allows the thorax skin to " continuously" deform in response to contact loading and spinal deformation.

VALIDATION OF THE MID SIZE MALE MODEL

The mid size male model has been validated extensively as shown in Table 1. Two major categories of tests were conducted: volunteer tests for low severity loading and post mortem human substitute (PMHS) tests for higher severity loading. Within these two categories, sled tests and blunt impactor tests have been used in various loading directions and for various body parts.

***Table 1**: Overview of validations performed with the mid size male human model,*
 # indicates the number of different test conditions within the severity range applied

Test set-up	Loading direction								
	Frontal			**Rear**			**Lateral**		
	Type	Severity	#	Type	Severity	#	Type	Severity	#
Whole body sled	Volunteer	3-15 g	3	Volunteer	4-5 g	2			
				PMHS	9 –12 g	3	PMHS	21, 37 g	2
Spine quasi-static	Volunteer		1	Volunteer		1			
Thorax impactor	PMHS	3-10 m/s	8				PMHS	3-6 m/s	2
Abdomen impactor	PMHS	6-9 m/s	2						
Shoulder impactor							PMHS	4-7 m/s	4
Pelvis impactor							PMHS	3-10 m/s	4

Validation for frontal loading can be found in Happee et al. (1998). Rearward validation is published by Happee et al. (2000) and further validation including volunteers on deformable seats is to be published. This paper focuses on the lateral validations, which have not been published elsewhere. The lateral PMHS full body sled test validations are described below. The frontal and lateral impactor validations from Table 1 are illustrated in Fig. 4 and loading conditions and validation results are shown in Appendix B. For some PMHS impactor corridors, corrections for muscle tone have been proposed in the literature. In these cases the corrected corridors have been applied, but for other tests such a correction had not been specified. As can be seen in Appendix B the model is generally close to the corrected corridors, and is generally somewhat stiffer than the uncorrected PMHS corridors.

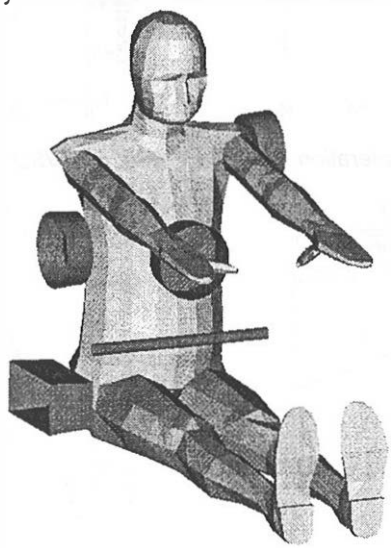

***Fig. 4**: Frontal impactor locations (thorax, abdomen) and lateral impactor locations (shoulder, thorax, pelvis), see further Appendix B.*

LATERAL PMHS SLED VALIDATION

Irwin et al. (1993, 1994) described lateral sled tests performed at Wayne State University using PMHS subjects distinguishing situations in which the cadaver impacts a padded wall and situations in which impact with a rigid wall takes place. Rigid wall impacts at 6.7 m/s with a peak sled acceleration of 20g and at 9.1 m/s with a peak sled acceleration of 37g have been investigated here. An impression of the kinematics of the 6.7 m/s, 20g impact is given in Fig. 5 and Figs 6-13 show the correlation with the corresponding experiments. Shoulder and spinal lateral accelerations and displacements have been plotted. Furthermore a summation of contact forces at the shoulder and upper thorax level has been derived from the contact forces with the two upper bars of the test set-up (Fig. 5).

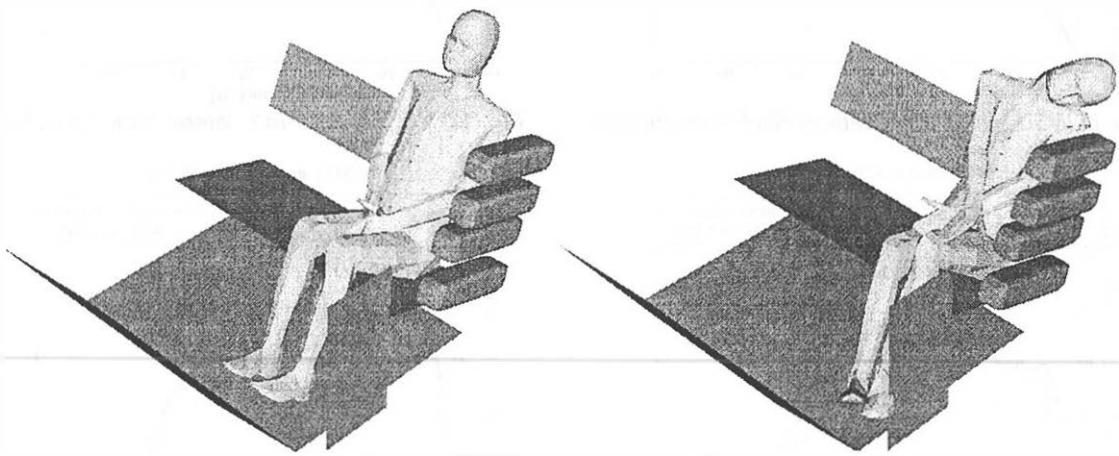

***Fig. 5**: Kinematics of WSU lateral whole body PMHS test, v = 6.7 m/s, 20g. t = 0 ms (left), t = 60 ms (right).*

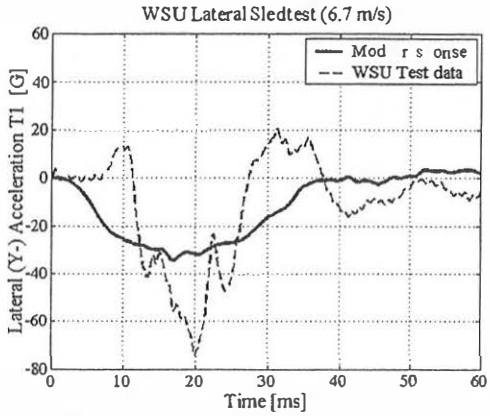

Fig. 6: WSU test 6.7 m/s, lateral acceleration T1.

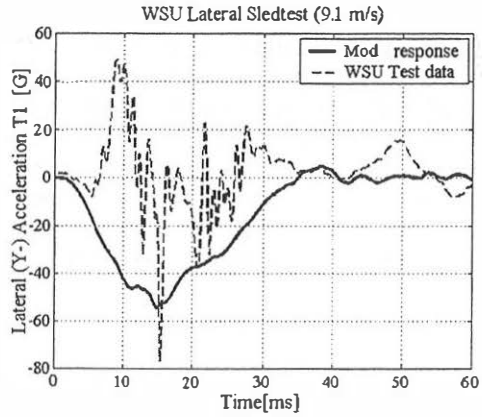

Fig. 10: WSU test 9.1 m/s, lateral acceleration T1.

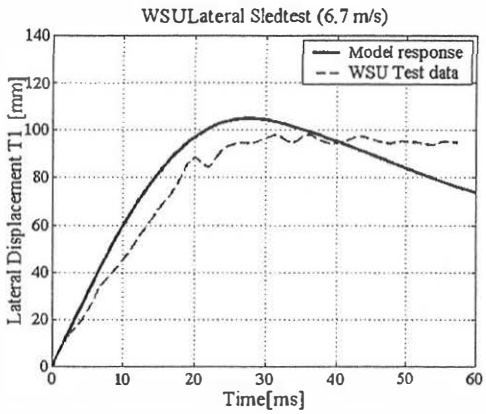

Fig. 7: WSU test 6.7 m/s, lateral displacement T1.

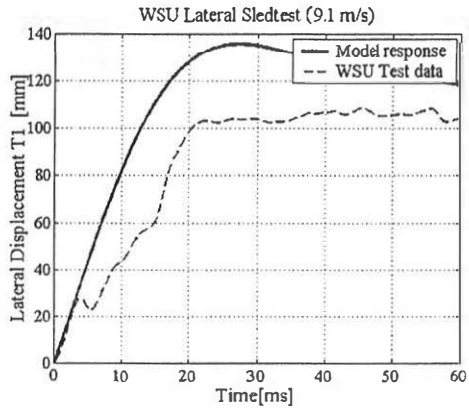

Fig. 11: WSU test 9.1 m/s, lateral displacement T1.

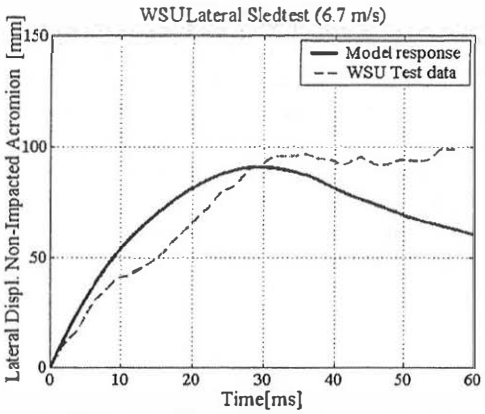

Fig. 8: WSU test 6.7 m/s, lateral displ. right shoulder.

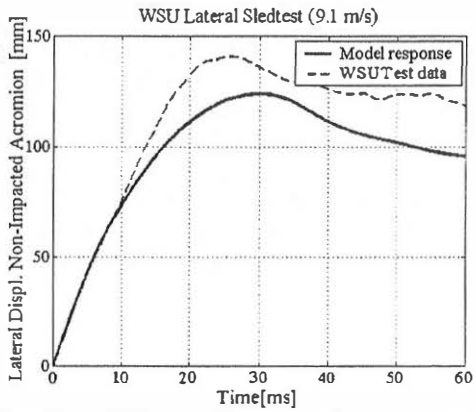

Fig. 12: WSU test 9.1 m/s, lateral displ. right shoulder.

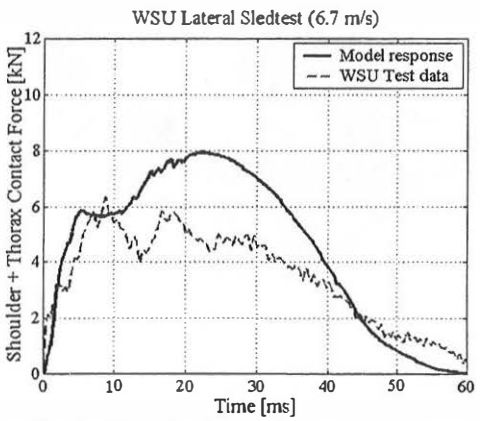

Fig. 9: WSU test 6.7 m/s, shoulder/thorax contact force.

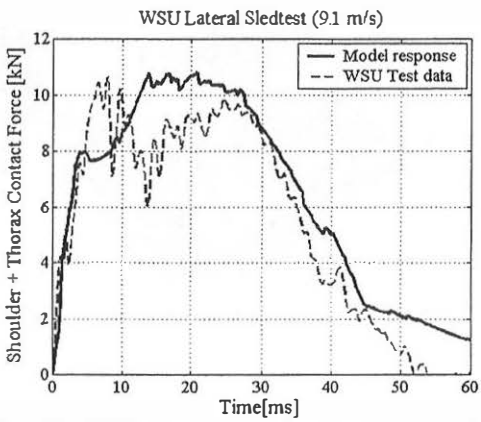

Fig. 13: WSU test 9.1 m/s, shoulder/thorax contact force.

VALIDATION OF THE SMALL FEMALE MODEL

The small female model has been validated using published small female impactor corridors for the SID2s dummy (Daniel et al., 1995). Results are given in Appendix C, and are comparable to results for the mid size male model in Appendix B. It should be noted that this validation of the small female model is actually a comparison of a scaled model to scaled biofidelity requirements. This validation with scaled requirements is included to relate the small female model to these published requirements as well as to the SID2s dummy. However a validation on experimental data with small human subjects as described below is more relevant.

SMALL FEMALE VALIDATION WITH DEPLOYING SIDE AIRBAG

Proliferation of inflatable restraint technology has occurred worldwide with both frontal and side impact airbags becoming common in most passenger vehicles. Concerns generated by small occupants in proximity to deploying airbags have been considered by PMHS testing (Kallieris et al., 1997) and by testing on dummies and PMHS (Duma et al., 1998). These concerns have prompted regulatory agencies and manufacturers to develop test procedures to determine injury potential based on airbag/occupant interaction.

For evaluation of side airbag interaction with small drivers (like 5th percentile females), a limited study of tests involving PMHS was carried out. The test procedures for the PMHS tests are described in Appendix D. Subsequent to the testing; the test conditions were replicated in a simulation using the small female human model and features of the MADYMO code to describe the side impact airbag module. The vehicle seat, occupant position, airbag mounting, airbag material, inflator mass flow and temperature, and airbag fold were used as initial inputs for the model. A static deployment of the airbag was achieved through initiation of the inflator mass flow. Occupant kinematics as well as sternum, clavicle, scapula, humerus and ulna accelerations were monitored throughout the deployment event as the airbag interacted with the occupant (see Appendix D). These output parameters were compared to PMHS recorded test data taken from the same positions on the subject.

The airbag mesh was generated from CAD drawings of actual design. The head/thorax side airbag mesh was folded using double tuck pattern in combination with accordion folds (see Fig. 14). The folding was done using HYPERMESH. The folded mesh was very carefully checked for any initial penetrations. The final folded mesh dimensions were compared with the actual folded airbag and corrected for any errors. The folded airbag was attached to the inflator housing as in reality. The airbag housing cover and seat foam were not included in the model. It was found through testing that the cover does not especially affect the airbag deployment forces. The seat foam was trimmed out at the module location to ensure clean bag deployment. In order to avoid the reverse direction deployment, one ellipsoid is placed just behind the airbag model. The real airbag has two chambers, whereas the MADYMO airbag model has six artificial chambers to represent the deployment of folded airbag. All chambers are separated by several 'HOLE' type elements, which do not cause force on cushion outer panels. The unfolding of the head/thorax airbag was conducted using jet effect to simulate the dynamic effect of the mass flow during the airbag inflation process. The gas velocity, density, direction of gas jet and temperature for the gas were calculated using MSC-DYTRAN. Thus, the mass flow rate, the temperature and the direction of the jet flow were defined as input for this simulation. The gas leakage through the airbag fabric was defined by a pressure dependent mass outflow rate curve.

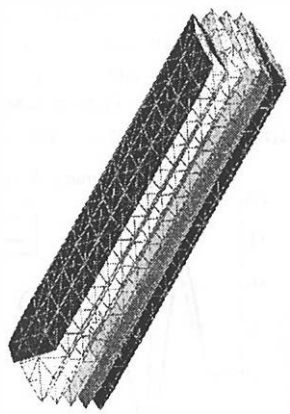

***Fig 14**: Folded F.E. airbag model.*

The folded head/thorax side airbag was validated with the use of a special series of airbag tests. The airbag module was attached to a test fixture with provisions to measure the reaction forces of the airbag module during deployment. Two tri-axial load cells were mounted at the top and the bottom of the back of the module. High-speed video cameras were used to capture in detail the kinematics of the unfolding airbag in different views.

Door and B pillar of the vehicle used in the PMHS tests were modelled using rigid body ellipsoids to consider the airbag contact. The most important area is where the door belt line meets the B pillar because the airbag has most contact with this part during deployment.

The simulation was built by integrating human body model, folded airbag, door, B pillar and seat. The human body model was positioned using photos of the tests (see Fig. 15). PMHS anthropometry is shown in appendix D. The PMHS had 9 kg more weight and 6 cm lower standing height than the human model (see Appendix A and D). However, since the shoulder height provided an adequate match, it was considered useful to compare the arm and shoulder part motions and acceleration trends of PMHS and human model to understand the validity of human body model.

Simulation results were compared with PMHS test number 2 (front right seat position) because the test number 1 (front left seat position) had some instrumentation errors. The MADYMO model was built for front left seat because the folded airbag model was built for left seat. It is not a problem to compare left and right seat positions since the model symmetry can be employed.

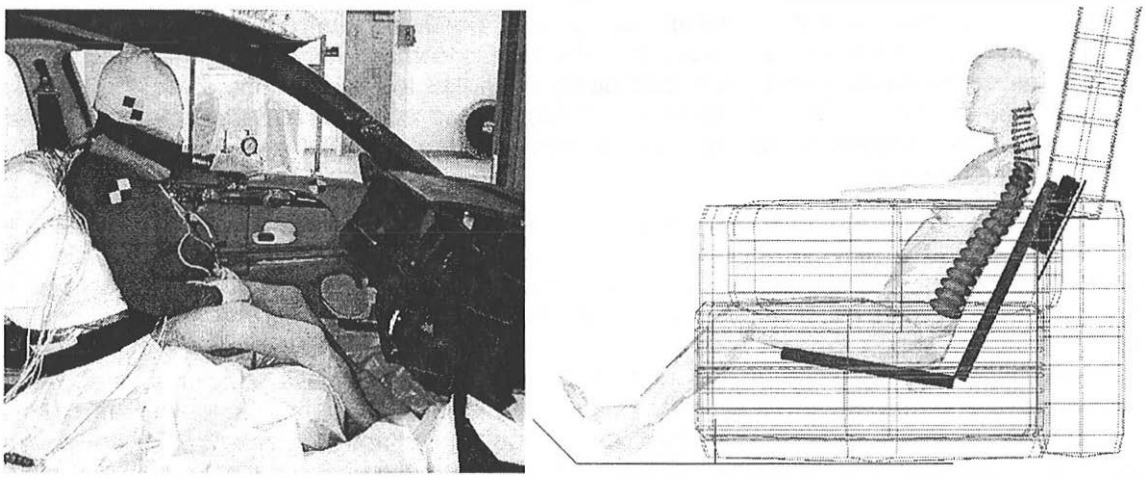

***Fig 15**: Small female PMHS side airbag test 1 and Integrated MADYMO Model.*

Animation comparisons on side and front view demonstrate very similar occupant arm and shoulder motions throughout the event (Fig. 21). The acceleration curves on sternum, clavicle, scapula, humerus and ulna are shown in Figs 16-20. They show good agreement for amplitude and duration at 0 to 10 msec but the number of peaks do not match throughout the event. It seems that several acceleration peaks from the PMHS test are caused by the step-by-step unfolding of the airbag. Because the airbag model does not simulate the exact step-by-step unfolding phenomena, the number of acceleration peaks does not match with the test. The secondary peaks of scapula acceleration from the simulation around 23 msec are caused by airbag rotation around the z-axis, which is not seen in the PMHS test. These secondary acceleration peaks are of less concern since initial punchout loading of the airbag (first 20 msec) is of most concern for injury.

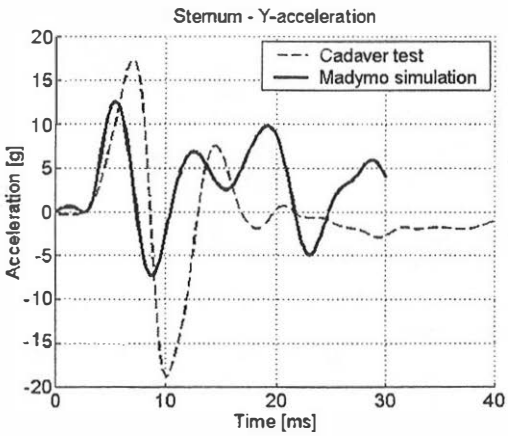

***Fig 16**: Airbag test, Sternum Y-acceleration.*

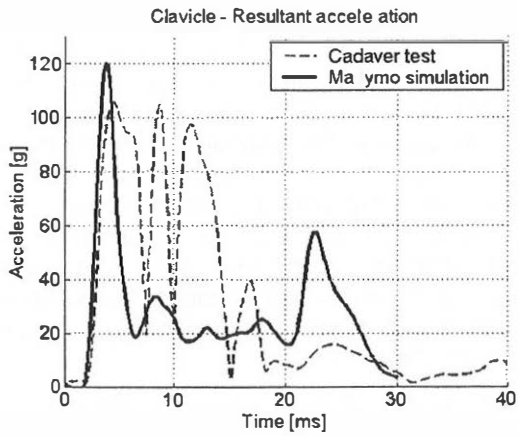

***Fig 17**: Airbag test, Clavicle resultant acceleration.*

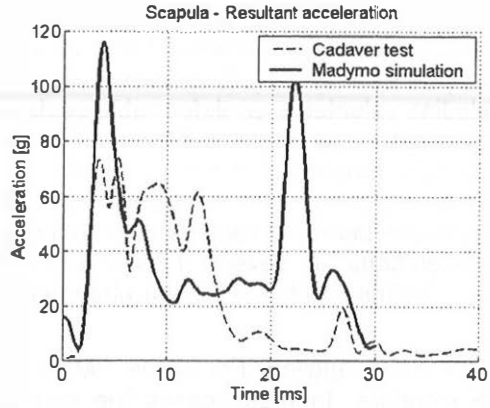

Fig 18: Airbag test, Scapula resultant acceleration.

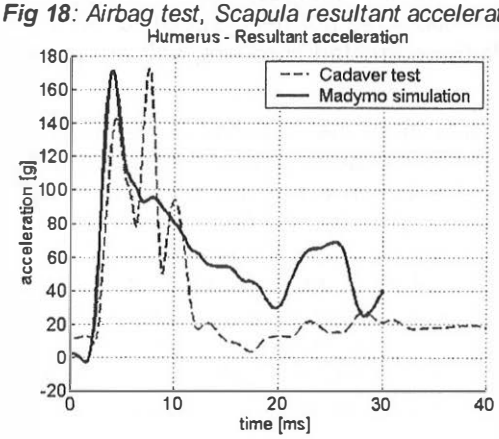

Fig 19: Airbag test, Humerus resultant acceleration.

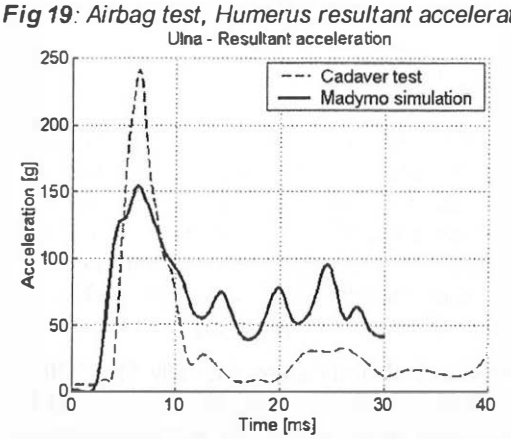

Fig 20: Airbag test, Ulna resultant acceleration.

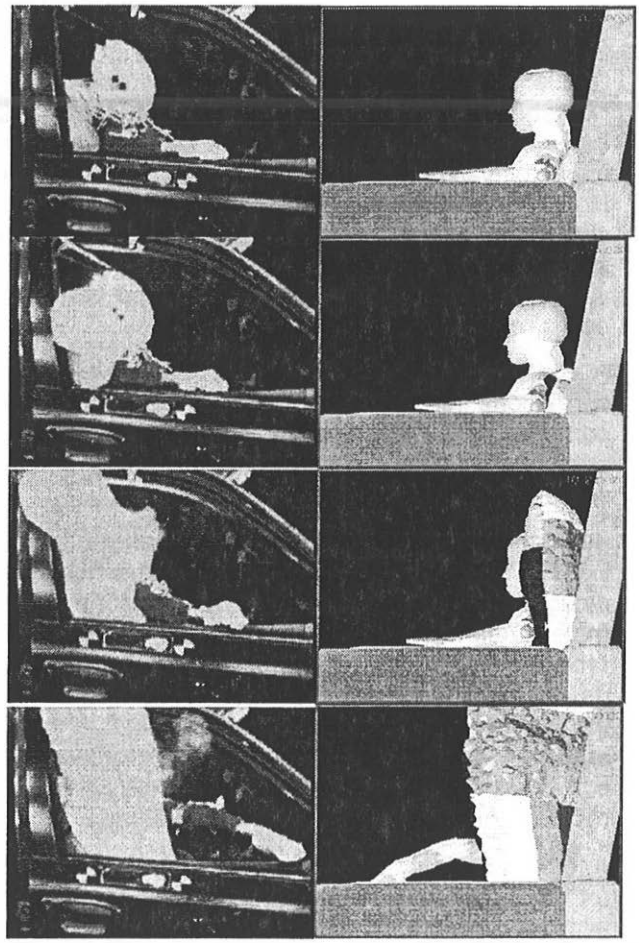

***Fig. 21:** Side airbag test, lateral view (0,5,10,22 ms).*

DISCUSSION

Human models in two body sizes have been developed and validated. The human geometry was derived from the RAMSIS anthropometric model, which provided a realistic surface description in particular for seated automotive postures. The model was extended for crash-simulations and validated for frontal, lateral and rearward loading. The model allows simulation of global injury criteria like chest-deflection, acceleration, and neck loads. For a more detailed analysis, submodels can easily be integrated into the current whole body model. The detailed lower leg model by Cappon et al. (1999) and the detailed neck model by van der Horst (1997) have already been integrated into the mid size male model.

Flexible bodies were applied in order to describe frontal and lateral compression of the rib cage, the abdomen and the pelvis. The flexible bodies describe global deformations while local deformation is described by the contact algorithm. The resulting capability to model torso deformation was found sufficient to match the available validation data.

The mid size male model was extensively validated using: frontal and rearward volunteer sled tests, frontal and lateral PMHS impactor tests in various body regions, lateral and rearward PMHS sled tests (Table 1). Validation for frontal loading can be found in Happee et al. (1998). Rearward validation is published by Happee et al. (2000) and further validation including volunteers on deformable seats is to be published. This paper describes lateral sled test validations and a complete set of frontal and lateral impactor validations as given in Appendix B. The small female model was validated using scaled biofidelity requirements from the literature and biomechanic data of the applicable body size including side airbag loading. Both models were found to satisfy the available biofidelity requirements in terms of kinematics, chest deflections, impactor forces, and accelerations at several locations. Further validation efforts will include oblique and vertical loading and further validation for the abdomen and pelvis region.

A combination of volunteer and PMHS validation sets have been applied. For some PMHS tests corrections for muscle tone have been proposed in the literature. In these cases the corrected corridors have been applied, but for other tests such a correction had not been specified. As can be seen in Appendices B&C the models are generally close to the corrected corridors, and are generally somewhat stiffer than the PMHS corridors.

It is important to know where the human model responses differ from the response of crash dummies like Hybrid III, Eurosid-1 and SID2s. The human models satisfy biofidelity requirements also used to design these dummies. Some comparisons were performed between the response of the mid size male human model and a Hybrid III model. In frontal airbag and/or belt loading, the human model provided larger chest deflections even though the human thorax model matches Hybrid III biofidelity requirements for blunt impact (Figs B3-B4). In the human model much more flexibility is observed in the lumbar as well as the cervical spine. A substantial torsion is observed in the torso making the human model more susceptible to shoulder belt roll out than the Hybrid III. These results are comparable to those of Baudrit et al. (1999) and indicate benefits of human models in simulating belt roll out. The spinal flexibility is of course also very important for simulation of rearward loading.

Another important benefit of the human models presented is the multi-directional biofidelity. The small female with side airbag simulation demonstrated good kinematic and arm/shoulder complex acceleration comparisons. This is a critical step in determining if models can be used to predict human injury response. The model has the ability to capture the acceleration response of the arm and shoulder during the first ten milliseconds of airbag contact when injury potential is greatest due to high punchout effects. Even though injury was not detected in the tests, the sub-threshold prediction has value to designers of side impact restraint systems. Future testing of out-of-position occupants in side impact conditions by automotive manufacturers will include using the 5th female (SID2s) in the elbow on window sill (beltline) position (ISO TR 15827 : Test Procedures for evaluating occupant interactions with deploying side airbags). Additional comparison of the model/PMHS data to SID2s (with instrumented arm) response may help distinguish when threshold levels of injury may occur.

The current crash-safety design is largely based on a limited set of body sizes (usually 5th, 50th and 95th percentile crash-dummies). Happee et al. (1998b) simulated frontal impacts with 30 different body sizes and found a wide range of results largely exceeding the range of results for standard dummies. These simulations were performed using "scaled dummy models". Using RAMSIS anthropometries a series of human body models of different sizes will be developed and validated using test data from biological specimens of varying anthropometry. This will allow, on the longer term, to base crash-safety design on real human body models taking into account the large anthropometry variations in current and future populations.

CONCLUSIONS

Multi-directional human models in two body sizes have been developed and validated. These models are considered a first step towards an omni-directional human model of variable body dimensions.

In the validations presented a satisfactory prediction has been obtained for kinematics, chest deflections, impactor forces, and accelerations in several body parts.

Recommendations include further development of the pelvis and abdomen model and further validation for different body sizes. In addition detailed segment models are being prepared retrofitting the current full body models.

Acknowledgement: The authors thank Masood Mohammed of TRW for his coordination of the PMHS testing for airbag side impact. They also thank Mr. Suk-Jae Ham of TNO-MADYMO North America for his assistance with the MADYMO modeling.

REFERENCES

1. Baudrit P., Hamon J., Song E., Robin S., Coz J. le (1999). Comparative studies of dummy and human body models behavior in frontal and lateral impact conditions. STAPP Conference 1999, Paper 99SC05.
2. Bouquet R., Ramet M., Bermond F., Cesari D., Thoracic and human pelvis response to impact, proceedings of the 14th International technical conference on enhanced safety of vehicules, 1994, pp. 100-109.
3. Cavanaugh J.M., Nyquist G.W., Goldberg S.J., King A. I. (1986). Lower abdominal tolerance and response, SAE Paper N° 861878.
4. Cappon H.C., Kroonenberg A.J. van den, Happee R., Wismans J. (1999). An improved lower leg multibody model. 1999 International IRCOBI Conference on the Biomechanics of impact, Sept 23-24, 1999, Sitges, Barcelona, Spain.
5. Daniel et al. (1995). Technical specifications of the SID-IIs Dummy. SAE paper 952735.
6. Duma S., Crandall J., Hurwitz, Pilkey W. (1998). Small female upper extremity interaction with a deploying side airbag. STAPP Conference, SAE 983148.
7. Engin A. (1980) On the biomechanics of the shoulder complex. Journal of Biomechanics, Vol.13, pp. 575-590.
8. Happee R., Hoofman M., Kroonenberg A.J. van den, Morsink P., Wismans J. (1998). A mathematical human body model for frontal and rearward seated automotive impact loading. STAPP Conference 1998, SAE 983150.
9. Happee R., Haaster R. van, Michaelsen L., Hoffmann R. (1998b). Optimisation of vehicle passive safety for occupants with varying anthropometry. ESV Conference 1998, Paper 98-S9-O-03.
10. Happee R., Meijer R., Ono K., Horst M.J. van der, Yamazaki K. (2000). Analysis of rear end impact using mathematical human modelling. JSAE spring convention 2000, JSAE paper No 20005335.
11. Huang Y., A.I. King, J.M. Cavanaugh (1994a). A MADYMO Model of Near-Side Human Occupants in Side Impacts. Journal of Biomechanical Engineering, vol. 116, may 1994, p.228-235.
12. Huang Y., A.I. King, J.M. Cavanaugh (1994b). Finite Element Modelling of Gross Motion of Human PMHSs in Side Impact. STAPP 1994, SAE 942207.
13. Horst M.J. van der, Thunnissen J.G.M., Happee R., Haaster R.M.H.P van. (1997). The influence of muscle activity on head-neck response during impact. STAPP Conference 1997.
14. Irwin A.L., Walilko T., Malhotra A., Zhu Y., king A. (1993). Displacement responses of the shoulder and thorax in lateral sled impacts. STAPP Conference 1993, SAE 933124.
15. Irwin A.L. (1994). Analysis and CAL3D Model of the Shoulder and Thorax Response of Seven PMHSs Subjected to Lateral Impacts. Ph.D. Thesis Wayne State University, 1994.
16. Irwin, A.L., Mertz H.J. (1997). Biomechanical bases for the Crabi and Hybrid III child dummies. SAE 973317, STAPP-1997.
17. Ishikawa H., Kajzer J., Schroeder G. (1993). Computer simulation of impact response of the human body in car-pedestrian accidents. Stapp Conference, 1993.
18. ISO-N455 (1996). Road Vehicles - Anthropomorphic side impact dummy - Lateral response requirements to assess the biofidelity of the dummy. ISO/TC22/SC12/WG5. Document N455, Revision 2, May 1996.
19. Jakobsson L., Norin H., Jernstrom C., et al. (1994). Analysis of different head and neck responses in rear-end car collisions using a new humanlike mathematical model. IRCOBI conference 1994 proc., pp. 109-125.
20. Kallieris D., Rizetti A., Mattern R., Jost S., Priemer P., Unger M. (1997). Response and vulnerability of the upper artm through side airbag deployment. STAPP Conference 1997, SAE 973323.
21. Koppens W.P., Lupker H.A., Rademaker C.W. (1993). Comparison of modelling techniques for flexible dummy parts. STAPP Conference 1993, SAE933116.
22. Kroell C. K., Schneider D. C. and Nahum M. , Impact Tolerance and response of the human thorax, SAE Paper N°710851, Proceedings of the 15th Stapp Car Crash Conference, 1971.
23. Kroell C. K., Schneider D. C. and Nahum M. , Impact Tolerance and response of the human thorax II, SAE Paper N°741187, Proceedings of the 18th Stapp Car Crash Conference, 1974.
24. Kroonenberg A. van den, Thunnissen J., Wismans J. (1997). A human model for low severity rear-impacts. IRCOBI conference, 1997.
25. Lizee E., Robin S., Song E., Bertholon N., Coz J. le, Besnault B., Lavaste. (1998). Development of a 3D finite element model ofthe human body. STAPP Conference 1998, SAE-983152.
26. Lobdell T.E., Kroell C.K., Schneider D.C., Hering W.E., Nahum A.M. (1973). Impact response of the human thorax, Human impact response, Plenum press, New York.
27. Ma D., Obergefell A., Rizer A. (1995). Development of human articulating joint model parameters for crash dynamics simulations. STAPP Conference 1995, SAE 952726.
28. MADYMO (1999). MADYMO Theory Manual Version 5.4. TNO Road-Vehicles Institute, Delft, The Netherlands.
29. Mertz H.J., Irwin A.L., Melvin J.W., Stalnaker R.L., Beebe M.S. (1989). Size weight and biomechanical impact response requirements for adult size small female and large male dummies. SAE-890756.
30. Meyer E., Bonnoit J. (1994). Le choc lateral sur l'epaule: mise en place d'un protocole experimental en sollicitation dynamique, memoire de dea, Laboratoire de biomechanique appliquee, Fuculte de Marseille, 1994.
31. Nahum M., Gadd C. W., Schneider D. C. and Kroell C. K. Deflection of the human thorax under sternal impact, SAE Paper N°700400, Proceedings of the International Automobile Safety Conference, Detroit, 1970.
32. Nahum M., Schneider D. C. and Kroell C. K., Cadaver skeletal response to blunt thoracic impact, SAE Paper N°751150, Proceedings of the 19th Stapp Car Crash Conference, 1975.
33. Neathery R. (1974). Analysis of chest impact response data and scaled performance recommendations. STAPP 1974, SAE 741188.
34. Prasad P., King A.I. (1974). An experimentally validated dynamic model ofthe spine. J Appl Mech, 1974, pp. 546-550.
35. Ratingen M.R., Twisk D., Schrooten M., Beusenberg M.C., Barnes A., Platten G. (1997). Biomechanically based design and performance targets for a 3-year old child crash dummy for frontal and side impact. SAE 973316. Child Occupant Protection Symposium 1997.
36. SAE-J1460-MAR85. Human mechanical response characteristics. SAE Information Report.

37. Talantikite Y., Bouquet R., Ramet H., Guillemot H., Robin S., Vioglio E. (1998), Human thorax behaviour for side impact: Influence of impact mass and velocities, ESV Paper 98-S7-O-03.
38. Yang J.K, Lovsund P. (1997). Development and validation of a human body mathematical model for simulation of car-pedestrian impacts. IRCOBI Conference 1997.

APPENDIX A: SELECTED RAMSIS ANTHROPOMETRY

RAMSIS models have been developed for several populations including Germany, USA/Canada, Japan/Korea. The German population was surveyed as described in Table A1. Age was one of the stratification variables, i. e. the age distribution was representative of the population age distribution. From this population a mid size male model and a small female model were generated using RAMSIS options as specified in Table A2. For the mid size male model simply medium typologies were selected for height, weight and sitting height. For the small female a very short and very slim model was selected in RAMSIS. The resulting body mass and sitting height were considered to be somewhat extreme also in comparison to the small female Hybrid III. This was resolved in a second step using the BODYBUILDER submodule of RAMSIS. The proportion and corpulence have been adapted by modification of the percentile values of their related key parameters, respectively sitting height and waist circumference. For the sitting height the percentile value was changed from 2.2% to 5.0%, the waist circumference changed from 14.9% to 18.0%.

Table A1. The RAMSIS German population survey.

country	Germany
period	1982-1984
number of females	3059
number of males	3052
age range	18-59

Table A2. RAMSIS anthropometry parameters selected.

parameter	Mid size male	Small female	remarks
Software	RAMSIS version 3.1	RAMSIS version 3.4	
Population	German, 1984	German, 1984	
Gender	Male	Female	
Age group (year)	18-70	18-70	
Standing height [m] Length Typology	1.74 medium	1.52 very short 5.9th percentile	Hybrid III 50th perc male ~ 1.72 m Hybrid III 5th perc female ~ 1.52 m
Weight [kg]	75.7 medium waist	49.8 18th percentile	Hybrid III 50th perc male ~ 77 kg Hybrid III 5th perc female ~ 49 kg
Sitting height [m] Proportion Typology	0.92 medium torso length	0.81 5th percentile	Hybrid III 50th perc male ~ 0.91 m Hybrid III 5th perc female ~ 0.81 m
shoe model	GINO	GINO	
hand model	Mitten like	Mitten like	the four fingers are merged
posture	Car	Car	provides realistic skin for seated car occupant
range of motion	Medium	Medium	normal range of motion selected for the joints

APPENDIX B. IMPACTOR VALIDATION OF THE MID SIZE MALE MODEL

Blunt impactor tests as presented in Table B1 have been used for validation of the thorax, abdomen, shoulder and pelvis regions. The impactors were modelled as rigid bodies that are guided in the impact direction. Impactor force-deflection signals have been used for monitoring the model performance because they are published for many tests. Further, for lateral thorax tests and lateral shoulder tests described by the ISO report (1996) force vs. time corridors have been used. For the lateral thorax test at 4.3 m/s and for the lateral pelvis tests also T1-y acceleration signals have been plotted. Since the impactor contacts three flexible bodies for the thorax tests and two for the abdomen test, displacement output was generated for all flexible bodies. However only the highest deflections were considered to be representative for the actual displacement. Force output has been determined by multiplying the impactor mass with the impactor acceleration.

Table B1. Impactor validation experiments for the mid size male model.

Body segment	Test number	Impact direction	Impactor mass (kg)	Impactor velocity (m/s)	Source
Thorax	1	Frontal	23.4	4.27	Neathery (1974)
	2	Frontal [1]	23.4	6.71	
	3	Frontal	23.4	3.4	Bouquet (1994)
	4	Frontal	23.4	5.8	
	5	Frontal	23.0	4.9	Kroell (1971, 1974, 1975), Nahum (1970, 1975)
	6	Frontal	23.4	6.9	
	7	Frontal	22.2	9.9	
	8	Frontal [2]	10.4	7.0	
	9	Lateral	23.4	3.3	Lizee (1998), Talantikite (1998)
	10	Lateral [1]	23.4	5.9	
	11	Lateral	23.0	4.3	ISO report (1996)
	12	Lateral	23.0	6.7	
Abdomen	13	Frontal	31.4	6.9	Cavanaugh (1986)
	14	Frontal	63.6	9.4	
Shoulder	15	Lateral	23.4	4.5	ISO report (1996)
	16	Lateral	23.4	5.5	Meyer (1994), Lizee (1998)
Pelvis	17	Lateral	23.4	3.46	Bouquet (1994)
	18	Lateral	23.4	6.66	

[1] *The model was tuned with respect to this corridor*
[2] *Subjects were supported with a rigid backrest*

Thorax impact

Frontal blunt impact tests at different energy levels were simulated based on corridors presented by Bouquet et al. (1994), Kroell et al. (1971, 1974), Nahum et al. (1970, 1975), Neathery (1974) and Lizee et al. (1998). For the *thorax frontal* impacts the target point of the impactor is the mid-sternum at the 4th intercostal space level. For the *thorax lateral* impacts the target point is centred on the thorax at T8-T9 level. The impactor for the thorax tests was a guided impactor with a flat and smooth interface in the shape of a disc with diameter 15cm with rounded edges. In the frontal tests described by Neathery (1974) the biofidelity of the chest to blunt-frontal mid-sagittal impact has been assured by performance guidelines that are based on the following approach. PMHS data was normalised, load levels were increased with 667 N to account for muscle tensing, and penetration was adjusted by subtracting 12.7 mm to indicate the internal sternum deflection. These requirements are accepted biofidelity requirements for crash dummies designed for frontal loading (SAE J 1460). In these tests the human body is placed in a sitting position on a flat, horizontal surface. The arms and legs are extended horizontally and parallel to the mid-sagittal plane. The subject is placed in a position such that the surface of the thorax on the centreline of the impactor is vertical. The longitudinal centreline of the impactor has the same vertical height as the mid-sternum and lies in the mid-sagittal plane of the subject. Kinematics of the frontal thorax impact with impactor mass 23.4 kg and speed 6.71 m/s and for the lateral thorax impact with impactor mass 23.4 kg and speed 5.9 m/s are presented in Figs. B1-B2. Force-deflection, force-time and acceleration-time plots of all thorax simulations with the experimental corridors have been presented in Figs. B3-B14. For the frontal thorax experiments (4.27 and 6.71 m/s) the penetration of the impactor in the human thorax at the centre of the impactor was about 10 mm which agrees with the previously mentioned biofidelity requirement (SAE J 1460). It should be noted that no correction of muscle activity has been performed for the determination of the corridors of Kroell and Bouquet, although this has been done for the Neathery tests, as has been mentioned earlier. The distinction between corridors that have been corrected for muscle activity and those that have not been corrected is visible in the plots. The response curves of tests described by Neathery are more in the lower part of the corridor whereas the curves of the other tests with non-corrected curves are situated more in the upper part of the corridor.

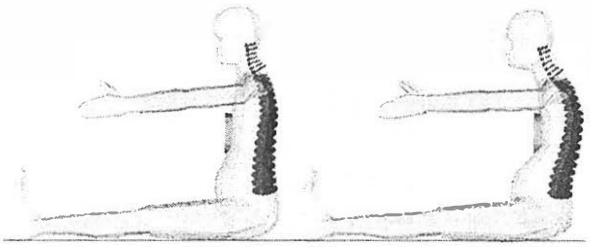

Fig. B1. Frontal thorax impact at t = 8 ms and t = 28 ms (max. deflection) after the initial impact. M= 23.4 kg, speed 6.7 m/s.

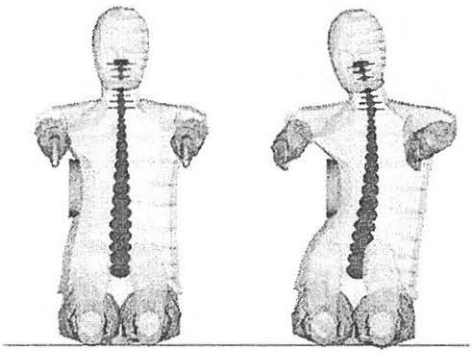

Fig. B2. Lateral thorax impact at t = 8 ms and t = 28 ms after the initial impact. M= 23.4 kg, speed 5.9 m/s.

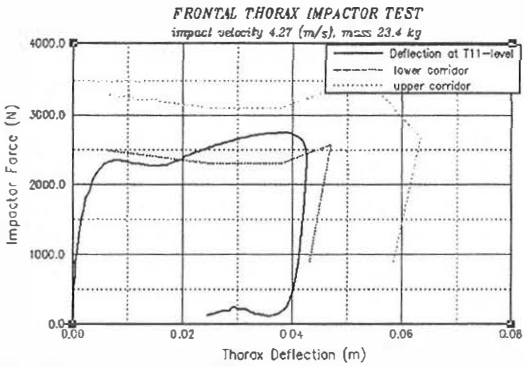

Fig. B3. Force-deflection for thorax frontal impactor test, v = 4.27 m/s, m = 23.4 kg, PMHS corridor corrected for muscle tone.

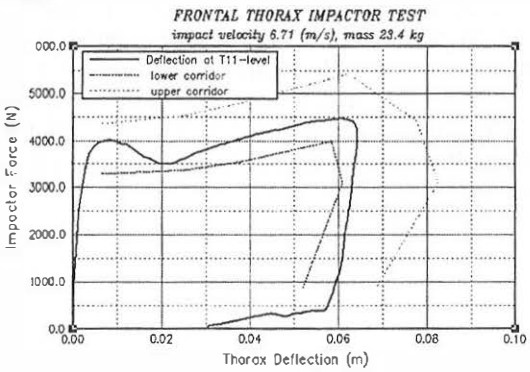

Fig. B4. Force-deflection for thorax frontal impactor test, v = 6.71 m/s, m = 23.4 kg, PMHS corridor corrected for muscle tone.

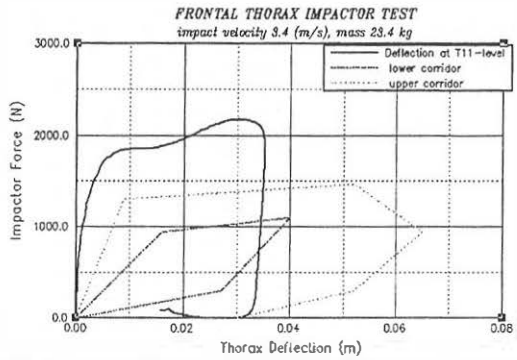

Fig. B5. Force-deflection for thorax frontal impactor test, v = 3.4 m/s, m = 23.4 kg, PMHS corridor not corrected for muscle tone.

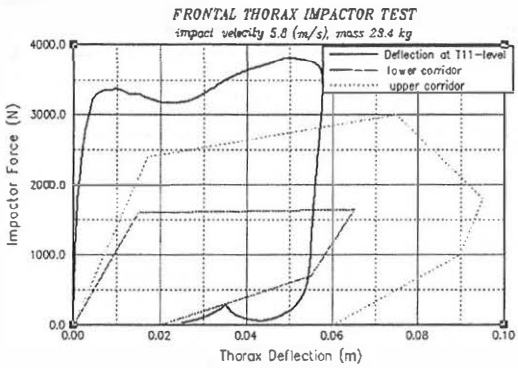

Fig. B6. Force-deflection for thorax frontal impactor test, v = 5.8 m/s, m = 23.4 kg, PMHS corridor not corrected for muscle tone.

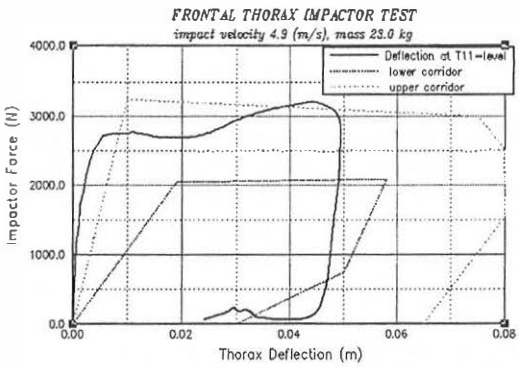

Fig. B7. Force-deflection for thorax frontal impactor test, v = 4.9 m/s, m = 23.0 kg, PMHS corridor not corrected for muscle tone.

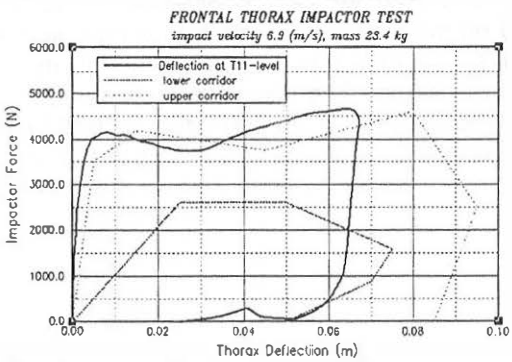

Fig. B8. Force-deflection for thorax frontal impactor test, v = 6.9 m/s, m = 23.4 kg, PMHS corridor not corrected for muscle tone.

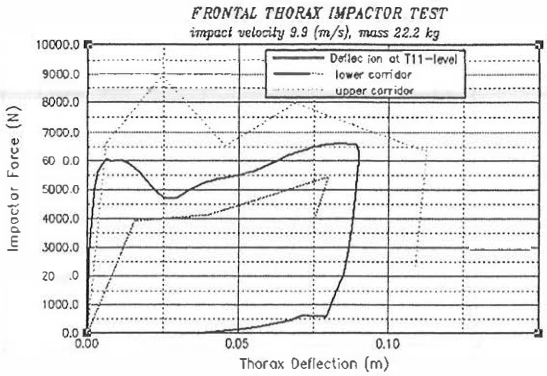

Fig. B9. Force-deflection for thorax frontal impactor test, v = 9.9 m/s, m = 22.2 kg, PMHS corridor not corrected for muscle tone.

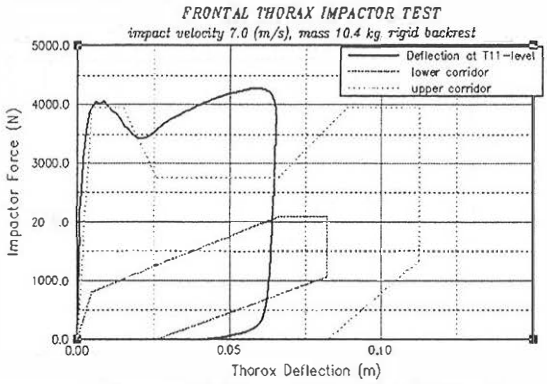

Fig. B10. Force-deflection for thorax frontal impactor test, v = 7.0 m/s, m = 10.4 kg, rigid backrest, PMHS corridor not corrected for muscle tone.

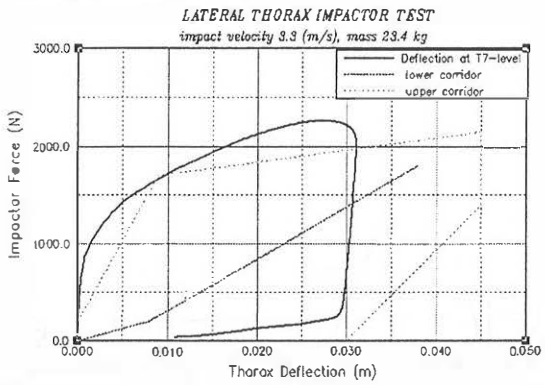

Fig. B11. Force-deflection for lateral impactor test, v = 3.3 m/s, m = 23.4 kg, PMHS corridor not corrected for muscle tone.

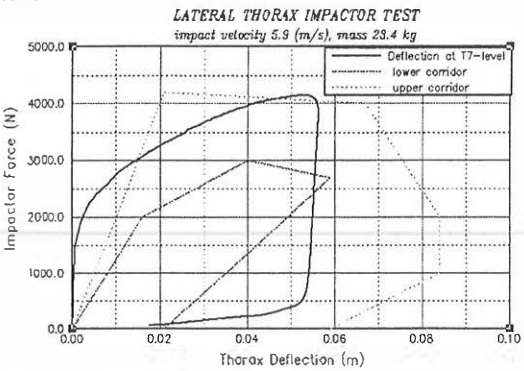

Fig. B12. Force-deflection for thorax lateral impactor test, v = 5.9 m/s, m = 23.4 kg, PMHS corridor not corrected for muscle tone.

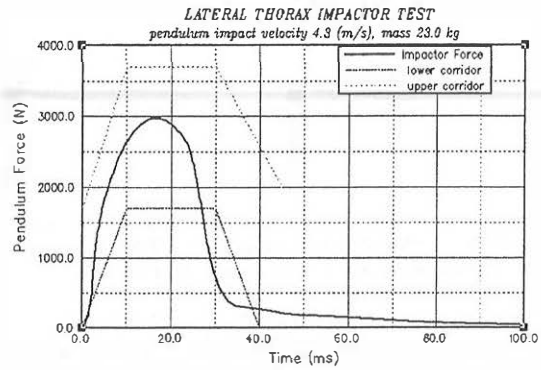

Fig. B13a. Force – time for thorax lateral impactor test, v = 4.3 m/s, m = 23.4 kg, PMHS corridor not corrected for muscle tone.

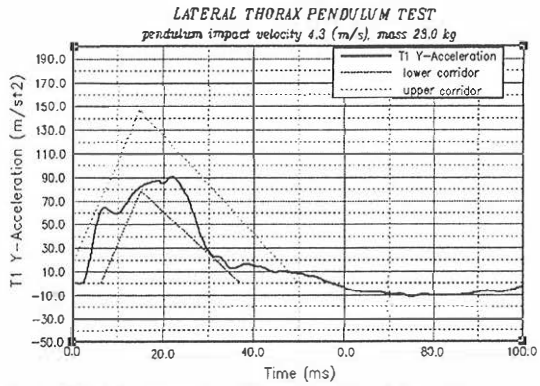

Fig. B13b. T1- y acceleration – time for thorax lateral impactor test, v = 4.3 m/s, m = 23.4 kg, PMHS corridor not corrected for muscle tone.

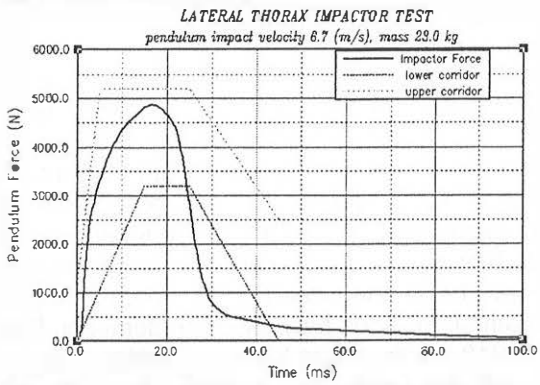

Fig. B14. Force – time for thorax lateral impactor test, v = 6.7 m/s, m = 23.0 kg, PMHS corridor not corrected for muscle tone.

Abdomen impact

The impactor for the *frontal abdomen tests* was also a guided impactor, an aluminium bar with diameter 25 mm and length 381 mm, that has been oriented in such a way that the long axis of the bar is parallel to the width of the human body. It was centred at L3 level (Cavanaugh et al., 1986). The kinematics of the frontal abdomen impact with impactor mass 31.4 kg and speed 6.9 m/s are presented in Fig. B15. The force-deflection for frontal abdomen impact is presented in Fig B16.

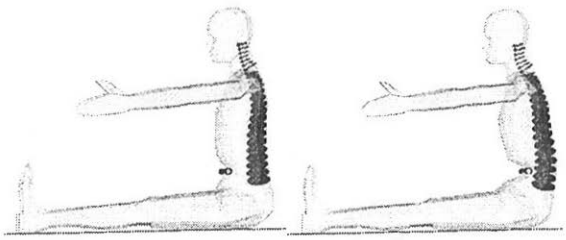

Fig. B15. Frontal abdomen impact at t = 8 ms and t = 24 ms after the initial impact. M= 31.4 kg, speed 6.9 m/s.

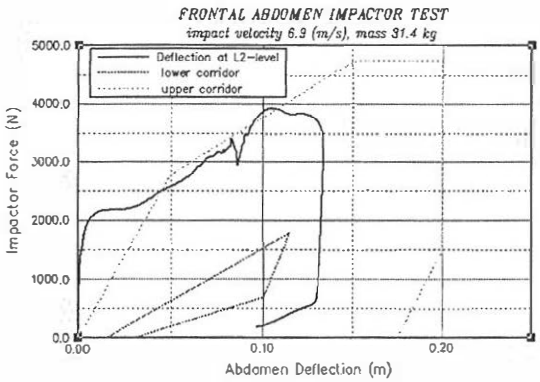

Fig. B16. Force-deflection for frontal abdomen impactor test, v = 6.9 m/s, m = 31.4 kg, PMHS corridor not corrected for muscle tone.

Shoulder impact

Lateral shoulder impactor tests have been performed with two types of impactors. In the experiment with impactor speed 4.5 m/s the same impactor has been used as described above for the thorax impactor tests. This test has been described in more detail in ISO report TC22/SC12/WG5 (1996). In the 5.5 m/s test however a square impactor with dimensions 0.1x0.1 m was applied. The axis of the impactor was aligned with the centre of the shoulder joint. This test has been described in more detail by Meyer (1994) and Lizee (1998). Force-time plots of both simulations have been presented in Figs. B17-B18. Furthermore for the shoulder impact at 4.5 m/s the peak displacement of the AC-joint with respect to T1 was 35 mm which is within the 34-41 mm biofidelity requirement with respect to shoulder displacement specified in the ISO report.

Pelvis impact

Lateral pelvis impacts at two energy levels have been described by Bouquet et al. (1994). For the first test no bone fracture was intended, for the second however a higher energy level was used to cause bone fracture. An impactor (mass 23.4 kg) with a rectangular impacting surface of 100 x 200 mm was guided towards the pelvis at the H-point. The force obtained at the tip of the impact hammer is presented in Figs. B19-B20.

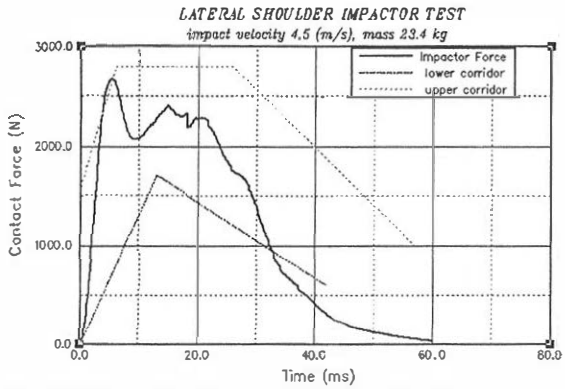

Fig. B17. Force-time for lateral shoulder impactor test, v = 4.5 m/s, m = 23.4 kg, PMHS corridor not corrected for muscle tone.

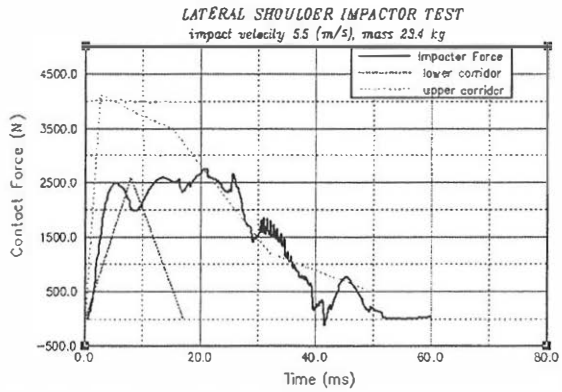

Fig. B18. Force-time for lateral shoulder impactor test, v = 5.5 m/s, m = 23.4 kg, PMHS corridor not corrected for muscle tone.

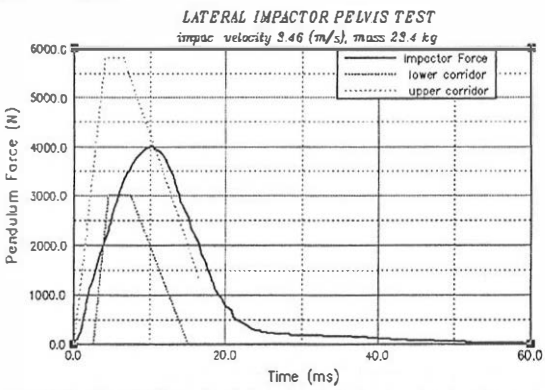

Fig. B19. Force-time for lateral pelvis impactor test, v = 3.46 m/s, m = 23.4 kg, PMHS corridor not corrected for muscle tone.

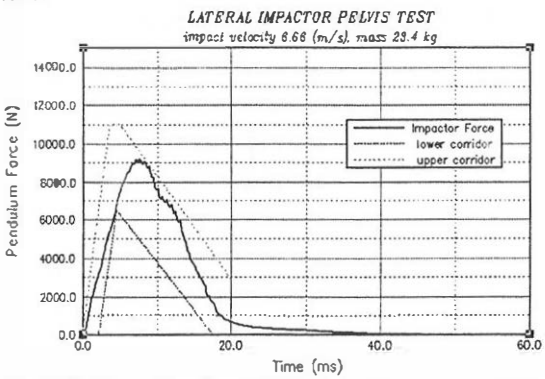

Fig. B20. Force-time for lateral pelvis impactor test, v = 6.66 m/s, m = 23.4 kg, PMHS corridor not corrected for muscle tone.

APPENDIX C. IMPACTOR VALIDATION OF THE SMALL FEMALE FEMALE MODEL

The small female model has been validated using published small female corridors for the SID2s dummy (Daniel et al. 1995). The performed simulations are presented in Table C1. The results together with the corridors are plotted in the Figures C1-C3.

Table C1. Impactor validation experiments for the small female model.

Body segment	Test number	Impact direction	Impactor mass (kg)	Impactor velocity (m/s)
Shoulder	1	Lateral	14.0	4.5
Thorax	2	Lateral	14.0	4.3
	3	Lateral	14.0	6.7

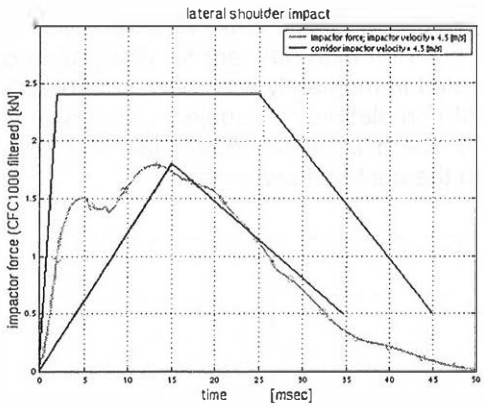

Fig. C1. Small female, force-time for lateral shoulder impactor test, v = 4.5 m/s, m = 14.0 kg, PMHS corridor corrected for muscle tone.

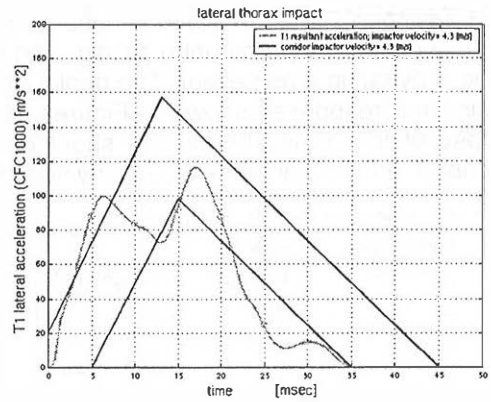

Fig. C2b: Small female, T1- y acceleration – time for thorax lateral impactor test, v = 4.3 m/s, m = 14.0 kg, PMHS corridor not corrected for muscle tone.

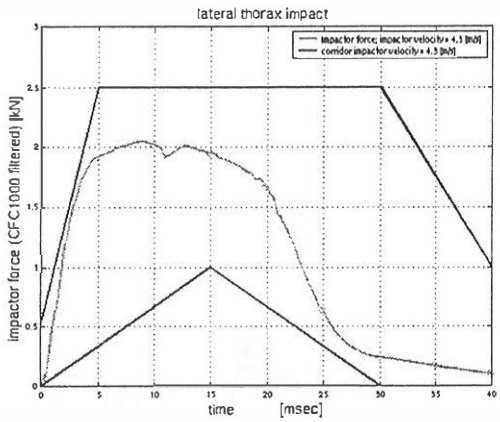

Fig. C2a. Small female, Force – time for thorax lateral impactor test, v = 4.3 m/s, m = 14.0 kg, PMHS corridor corrected for muscle tone.

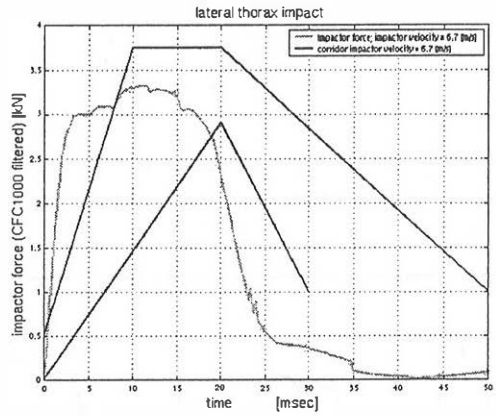

Fig. C3. Small female force – time for thorax lateral impactor test, v = 6.7 m/s, m = 14.0 kg, PMHS corridor corrected for muscle tone.

APPENDIX D. SIDE AIRBAG PMHS EXPERIMENTS

A generic, re-inforced large car body-in-wide was used to hold a production seat in both the driver and passenger position. Seats were fitted with generic head/thorax bag modules and the seat seams were opened to ensure consistent bag deployment. Eigth tests were performed on four post-mortem human subject testing both left and right sides on each subject. The tests conditions are given in Table D1 where parameters identical in all tests are given in Table D2. The arm positions are illustrated in Fig. D1.

Visual targets were placed on the subject's clavicle, humerus, ulna, and sternum for later film analysis. Triaxial accelerometers were placed on the lower humerus, lower ulna, lateral clavicle, lateral scapula, and T2 and T12 vertebral bodies. Additional accelerometers were placed on the upper sternum and lateral ribs (4 and 8). The humerus and clavicle were fitted with strain gages at mid position.

Upon arranged signal, the module inflator (peak output at 200 kPa in 28L tank) was deployed to fill a 20L fully coated (impermeable) airbag. The airbag has one 12mm external vent for dissipation of gas during a dynamic crash event. The deploying airbag interacted immediately with the test subject's arm causing the responses shown in Figures 16-20. Upon test completion, the subjects underwent a full autopsy of the arms, thorax and shoulder complex by a board certified pathologist. For the tests described, no bone or soft tissue injury was detected during the post test examination.

Table D1. Side airbag PMHS experiments

Test	Body side loaded	Subject			Arm Position	Air bag
		Height [m]	Weight [kg]	Age		
1	left	1.46	58.0	77	Beltline Fig D1-left	Head/thorax
2	right	1.46	58.0	77		Head/thorax
3	left	1.75	56.0	87	Armrest rearward Fig D1-mid	Head/thorax
4	right	1.75	56.0	87		Head/thorax
5	left	1.56	67.0	84		Thorax
6	right	1.56	67.0	84		Thorax
7	left	1.63	50.0	86	Armrest lateral Fig D1-right	Thorax
8	right	1.63	50.0	86		Thorax

* parameters will be given in final paper

Table D2. Side airbag PMHS experiments, common conditions

Parameter	Condition
Seat position	mid
Seat pan position	mid
Seat back angle	24 degrees measured at the seat back
Head rest position	Down
Seat bracket	45 degrees
Squib fire time	0
Belts	N/a

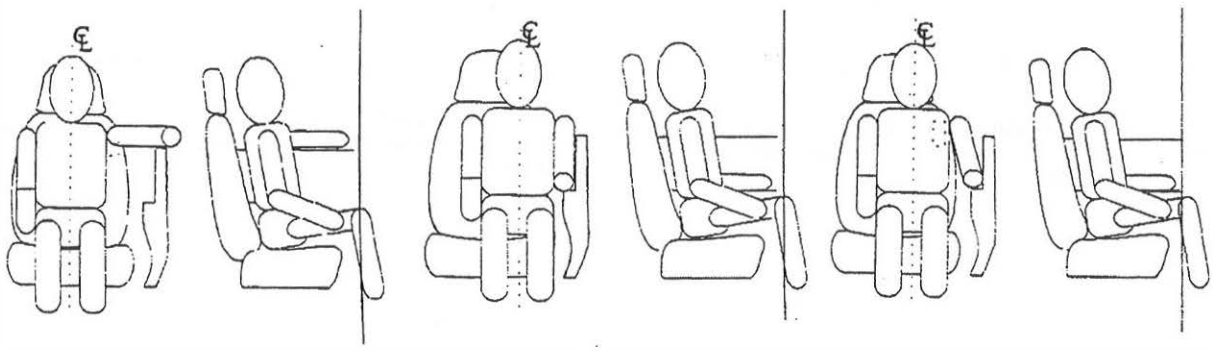

Fig D1. Arm and body positions: Beltline (left), Armrest rearward (mid), Armrest Lateral (right)